PAPER

# Modulating the bandgaps of graphdiyne nanoribbons by transverse electric fields

IOP PUBLISHING JOURNAL OF PHYSICS: CONDENSED MATTER
J. Phys.: Condens. Matter **24** (2012) 165301 (5pp) doi:10.1088/0953-8984/24/16/165301

# Modulating the bandgaps of graphdiyne nanoribbons by transverse electric fields

**Jun Kang[1,2], Fengmin Wu[1] and Jingbo Li[1,2]**

[1] Research Center for Light Emitting Diode, Zhejiang Normal University, Jinhua 321004, Zhejiang Province, People's Republic of China
[2] State Key Laboratory of Superlattices and Microstructures, Institute of Semiconductors, Chinese Academy of Sciences, PO Box 912, Beijing 100083, People's Republic of China

E-mail: jbli@semi.ac.cn

Received 26 October 2011, in final form 13 February 2012
Published 26 March 2012
Online at stacks.iop.org/JPhysCM/24/165301

**Abstract**
The effect of external transverse electric fields on the bandgaps of graphdiyne nanoribbons is investigated from first-principles calculations. The giant Stark effect is observed in the ribbons. When the field is applied, the valence and conduction band edge states are found to be strongly localized at low and high potential edges of the ribbon, respectively. Due to the wavefunction localization, the bandgap decreases with increasing field strength, and a semiconductor–metal transition occurs below a threshold field value. It is also shown that the bandgap decreasing rate depends linearly on the ribbon width. The tunable bandgap of a graphdiyne nanoribbon under an electric field would be helpful for practical applications.

(Some figures may appear in colour only in the online journal)

## 1. Introduction

In the past few years, there have been numerous investigations focused on the area of new carbon allotropes [1]. Since the 1980s, many new carbon allotropes, such as fullerenes [2], carbon nanotubes [3] and graphene [4] have been synthesized. More recently, graphdiyne [5, 6], a new kind of carbon allotrope which contains both sp- and $sp^2$-hybridized carbon atoms, has been successfully prepared on a Cu surface by a cross-coupling reaction using hexaethynylbenzene [7]. Through an anodic aluminum oxide template catalyzed by a Cu foil, graphdiyne nanotube arrays have also been generated later [8]. These experimental progresses have triggered many theoretical studies on graphdiyne and its related structures [9–13]. Among these structures, graphdiyne nanoribbons (GDNRs) have attracted considerable interest. For instance, Long *et al* expect that the electron mobility of GDNR can reach $10^4$ $cm^2$ $V^{-1}$ $s^{-1}$ [12], while Pan *et al* showed that the bandgap of GDNR increases with decreasing ribbon width [13]. The bandgap modulation of nanostructures is of importance for their applications. To achieve this goal, many methods have been suggested, such as size control [14, 15] and strain engineering [16–18], as well as electric field modulation. Previous studies have demonstrated that a transverse electric field can induce the giant Stark effect in one-dimensional materials, causing the bandgap to decrease or even vanish [19–22]. This effect has been confirmed experimentally in BN nanotubes [23] and carbon nanotubes [24]. Moreover, compared with other approaches to modify the bandgap, experimentally the control of an electric field is much easier. Hence one can expect that applying a transverse electric field can be a possible way to modulate the bandgaps of GDNRs.

In this work, we perform first-principles calculations to investigate the effect of electric fields on the band structures of GDNRs and we show that the bandgap decreases as the electric field strength increases due to the strong localization of band edge states under the field. The bandgap decreasing rate is found to be linearly dependent on the ribbon width. These findings confirm the prospect that the bandgaps of GDNRs can be tuned by electric fields.

## 2. Methods

Figure 1 shows the structure of GDNRs considered in this work. According to their edge shapes, the GDNRs can be classified as armchair type (AGDNR) or zigzag

 

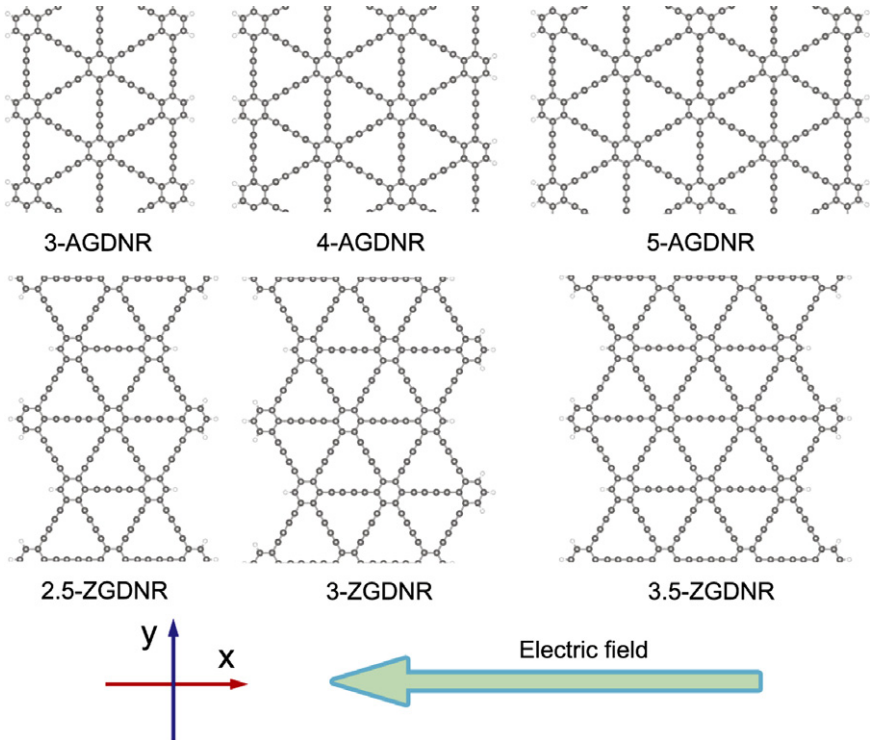


**Figure 1.** The structures of armchair and zigzag graphdiyne nanoribbons. Following [13], the nanoribbons are labeled according to the number of chains of hexagonal carbon rings.

type (ZGDNR). Following [13], the GDNRs are denoted as *n*-AGDNR or *n*-ZGDNR, where *n* is the number of chains of hexagonal carbon rings along the transverse axis. For AGDNR, *n* is an integer, whereas for ZGDNR, *n* can be either integer or half-integer. The constructed GDNRs are parallel to the *x*–*y* plane and periodic in the *y* axis. A vacuum layer of 11 Å is added along the *x* and *z* axes to avoid an interaction between adjacent ribbons. All edge atoms are passivated by H atoms. The scheme of Neugebauer and Scheffler is used to simulate an electric field [25]. The field is applied along the $-x$ direction. The width of GDNR is estimated by $w = \sqrt{3}Na^2/36c$, where $a$ is the lattice constant of a 2D graphdiyne sheet, which is calculated to be 9.456 Å, $c$ is the lattice constant of the GDNR and $N$ is the number of carbon atoms in the supercell.

The calculations are performed using the frozen-core projector augmented wave method [26, 27] as implemented in the Vienna *ab initio* simulation package [28, 29]. The generalized gradient approximation of Perdew–Burke–Ernzerhof [30] is adopted for the exchange–correlation functional. The cutoff energy for the plane wave expansion is 400 eV and the convergence criteria for the total energy is set to $10^{-5}$ eV. All atoms are relaxed until the calculated force on each atom is smaller than 0.02 eV Å$^{-1}$. The Brillouin zone is sampled by a $1 \times 7 \times 1$ mesh for AGDNR, while a $1 \times 5 \times 1$ mesh is used for ZGDNR.

## 3. Results and discussion

First we examine the bandgaps of GDNRs without an external electric field. The results are plotted in figure 2. The calculated bandgaps are in good agreement with those in [13]. Both AGDNRs and ZGDNRs have a direct gap at the Γ-point, and the gap value becomes larger as the ribbon width decreases, which results from the quantum confinement effect. Furthermore, it can be observed that the quantum confinement effect in ZGDNR is much stronger than that in AGDNR. In addition, the larger gap of ZGDNR can also be understood in view of the zone-folding model [31, 32]. According to the zone-folding model, the band structures of GDNRs can be regarded as the superposition of the graphdiyne electronic energy bands along the corresponding allowed $k$ lines, which are called 'slices'. These slices are parallel in the $k$ space and the distance between two adjacent slices is determined by the ribbon width. A larger ribbon width leads to a smaller distance. For AGDNR, the slices are perpendicular to the Γ–M direction, and for ZGDNR, the slices are perpendicular to the Γ–K direction. Because the direct bandgap of 2D graphdiyne locates at the Γ-point [6], the bandgap of GDNR is then determined by the slice which is closest to the Γ-point. Since the separation between the lowest conduction band and the highest valence band along the Γ–K direction is larger than that along the Γ–M direction in 2D graphdiyne [6], the slices perpendicular to the Γ–K direction would have larger gaps than those along the Γ–M direction (if the adjacent slice distances are similar for the two cases). As a result, bandgaps in ZGDNRs would be larger than those in AGDNRs with similar widths.

The calculated bandgap values can be fitted using the expression $E_g^{\text{ribbon}} = \beta/w^{\alpha} + E_g^{\text{sheet}}$, where $w$ is the width of the GDNR and $E_g^{\text{sheet}}$ is the bandgap of the 2D graphdiyne

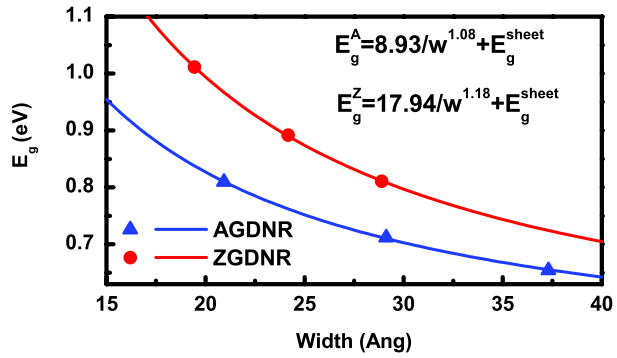


**Figure 2.** The bandgaps as a function of ribbon width for AGDNR and ZGDNR. The gap of a 2D graphdiyne sheet is 0.48 eV. Solid lines are fitting results.

sheet (0.48 eV according to our calculation). For AGDNR, we obtain $\alpha = 1.08$ and $\beta = 8.93$, whereas for ZGDNR we get $\alpha = 1.18$ and $\beta = 17.94$. In both types of GDNRs, $\alpha$ is close to 1, i.e. the bandgap difference $E_g^{ribbon} - E_g^{sheet}$ varies almost linearly with respect to the reciprocal of ribbon width. This is similar to the case of graphene nanoribbons [14].

Next we explore the effect of an external transverse electric field on the electronic properties of GDNRs. Here we take 4-AGDNR and 3-ZGDNR as examples, since other GDNRs exhibit similar trends. Figures 3(a) and (b) give the band structure of 4-AGDNR and 3-ZGDNR under a transverse electric field with different field strengths. It is clearly seen that the field affects the band structure significantly. For 4-AGDNR, the valence band maximum (VBM) and conduction band minimum (CBM) remain at the Γ-point under the field, but with increasing field strength, the VBM and CBM move towards each other and the bandgap decreases. When the field reaches about 0.055 V Å$^{-1}$, the VBM and CBM coincide and the bandgap closes, indicating a semiconductor–metal transition. For 3-ZGDNR, when the electric field is applied, its VBM and CBM move towards the X-point. Except for the position of VBM and CBM, the behavior of the bandgap of 3-ZGDNR under an electric field is similar to the case of 4-AGDNR. It becomes smaller when the field strength increases and the threshold strength for the semiconductor–metal transition is about 0.11 V Å$^{-1}$. The decreasing bandgap with increasing field strength originates from the redistribution of the wavefunction of the nanoribbon under an external electric field, namely the so called giant Stark effect (GSE) [19]. The VBM and CBM wavefunctions for 4-AGDNR and 3-ZGDNR with and without imposing an electric field are shown in figures 3(c) and (d), respectively. If no electric field is applied, the VBM and CBM wavefunctions distribute uniformly over the whole ribbon. The influence of an electric field on the wavefunction distribution is remarkable. The field mixes the

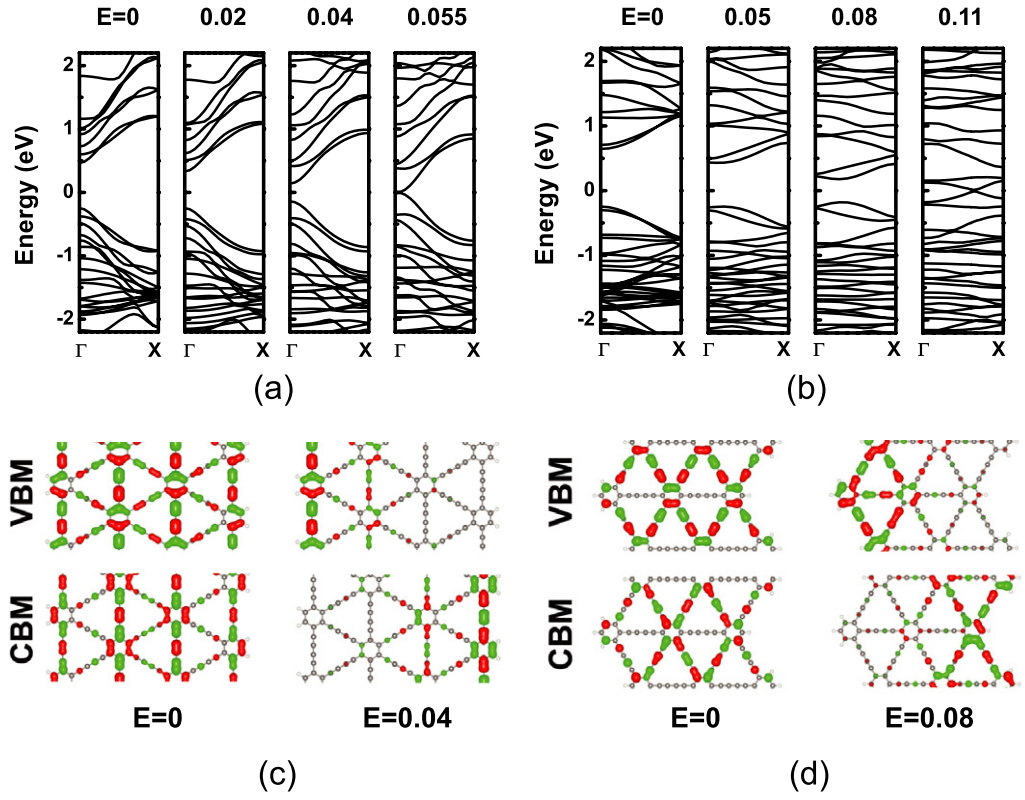


**Figure 3.** (a) The band structure of 4-AGDNR under electric fields with different strengths. (c) VBM and CBM wavefunction distributions of 4-AGDNR with and without electric fields. The isosurfaces correspond to 20% of the maximum values. (b), (d) The same as (a) and (c) for 3-ZGDNR. The unit of electric field is V Å$^{-1}$.

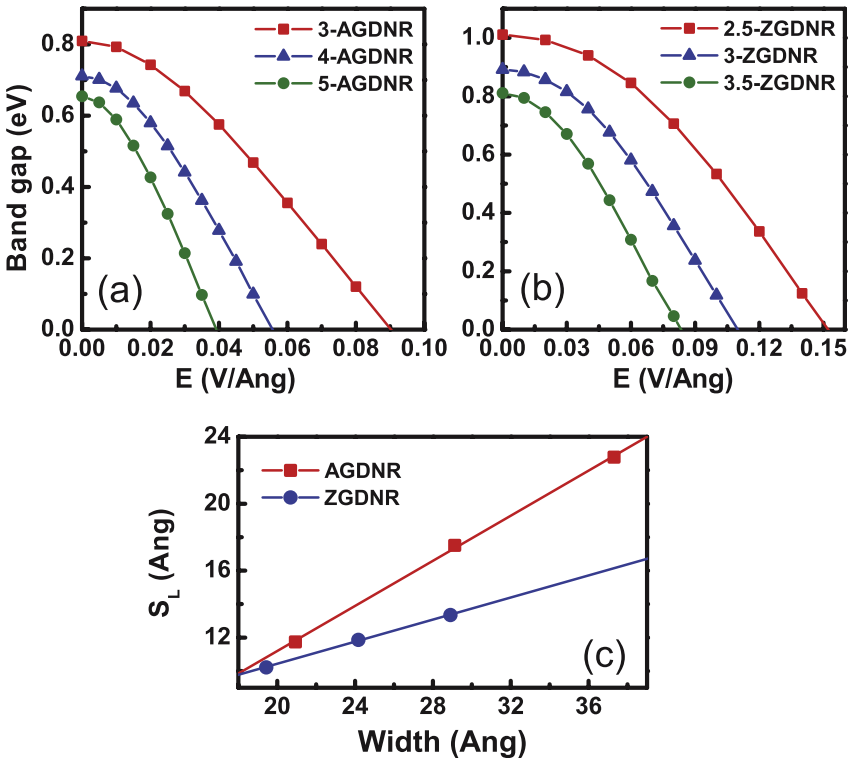


**Figure 4.** (a), (b) The bandgaps of AGDNRs and ZGDNRs as a function of electric field strength, respectively. The data points are extrapolated linearly to zero bandgap to estimate the threshold strength for the semiconductor–metal transition. (c) The GSE coefficient $S_L$ versus ribbon width for AGDNR and ZGDNR. Solid lines are fitting results.

subband states within the valence band complex or conduction band complex, leading to a redistribution of VBM and CBM wavefunctions. The VBM wavefunction moves along the same direction as the field, while the CBM wavefunction moves along the opposite direction. More importantly, the VBM and CBM wavefunctions are strongly localized at the edge of the ribbon. The VBM state localizes at the low potential edge and its energy increases. Whereas the CBM state localizes at the high potential edge and thus its energy decreases. As the field strength increases, the magnitude of the corresponding energy increase or decrease becomes larger and larger. Hence the bandgap decreases and finally vanishes.

To further analyze how the bandgap depends on the width and orientation of the GDNRs, we plot the bandgaps of different AGDNRs and ZGDNRs as a function of electric field strength in figures 4(a) and (b). The bandgaps of all GDNRs decrease monotonically when the electric field strength increases and a semiconductor–metal transition would happen below a threshold value. It should be noticed that, due to the underestimation of the bandgap using GGA, the threshold strength in figure 4 is also underestimated. However, this does not affect the general trend. When the field is weak, the bandgap decreasing rate is slow. However, as the field strength increases, the bandgap exhibits a linear response to the field. This happens because the VBM and CBM states are localized at the edge of the ribbon when the field is large, and their potential energy difference increases linearly with respect to the electric field. Consequently a linear dependence of the bandgap versus the electric field is observed. The slope $S_L$ of this linear region is defined as the GSE coefficient [33], which renders the capability of an electric field to modify the bandgap. The larger $S_L$ the material has, the more easily its bandgap can be tuned by the electric field. From figure 4 it can be seen that the $S_L$ strongly depends on the width of the ribbon. A ribbon with a larger width has a larger $S_L$. Zhang *et al* have investigated the scaling law of $S_L$ and they conclude that $S_L$ increases linearly with the ribbon width [33]. This can easily be understood since the potential energy difference between the localized VBM and CBM states under a certain electric field increases linearly with respect to the ribbon width. The $S_L \sim w$ plot for GDNR is presented in figure 4(c). Indeed, $S_L$ linearly depends on the ribbon width. Thus one can conclude that the bandgap of a wider GDNR is more sensitive to the electric field, and it can be expected that a semiconductor–metal transition in a sufficient wide GDNR can be observed under an experimentally achievable field strength. In addition, the slope $dS_L/dw$ strongly depends on the orientation of GDNRs. For AGDNR, the slope is 0.67, whereas for ZGDNR it is only 0.33. Hence the bandgap modulation in AGDNR would be easier than in ZGDNR. Both slopes are not equal to 1, which is in contrast to the case of BN nanoribbon or nanotube [33], indicating a screening of the electric field in GDNRs. What's more, the screening in ZGDNR is stronger than that in AGDNR as the slope for ZGDNR is much smaller.

## 4. Conclusions

In summary, we have investigated the effect of an external transverse electric field on the bandgaps of GDNRs from first-principles calculations. We show that the bandgap is tunable under an electric field. The gap decreases with increasing field strength and a semiconductor–metal transition happens below a threshold value. A larger ribbon width leads to a larger decreasing rate. The bandgap reduction originates from the localization of VBM and CBM states of the ribbon induced by the field, namely the giant Stark effect. These results provide a possible way to modify the bandgaps of GDNRs, which would be helpful for practical applications of GDNRs in the future.

## Acknowledgments

JL gratefully acknowledges financial support from the 'One-Hundred Talents Program' of the Chinese Academy of Science and National Science Fund for Distinguished Young Scholar (grant no. 60925016). This work is supported by the National Basic Research Program of China (grant no. 2011CB921901). The wavefunction plots are drawn with the help of the vaspmo program developed by Yang Wang. We acknowledge the computing resources provided by the Supercomputing Center, CNIC, CAS.

## References

[1] Hirsch A 2010 *Nature Mater.* **9** 868
[2] Kroto H, Heath J, O'Brien S, Curl R and Smalley R 1985 *Nature* **318** 162
[3] Iijima S 1991 *Nature* **354** 56
[4] Novoselov K S, Geim A K, Morozov S V, Jiang D, Zhang Y, Dubonos S V, Grigorieva I V and Firsov A A 2004 *Science* **306** 666
[5] Haley M M, Brand S C and Pak J J 1997 *Angew. Chem. Int. Edn* **36** 836
[6] Narita N, Nagai S, Suzuki S and Nakao K 1998 *Phys. Rev.* B **58** 11009
[7] Li G, Li Y, Liu H, Guo Y, Li Y and Zhu D 2010 *Chem. Commun.* **46** 3256
[8] Li G, Li Y, Qian X, Liu H, Lin H, Chen N and Li Y 2011 *J. Phys. Chem.* C **115** 2611
[9] Zhang H, Zhao M, He X, Wang Z, Zhang X and Liu X 2011 *J. Phys. Chem.* C **115** 8845
[10] Zhou J, Lv K, Wang Q, Chen X S, Sun Q and Jena P 2011 *J. Chem. Phys.* **134** 174701
[11] Luo G, Qian X, Liu H, Qin R, Zhou J, Li L, Gao Z, Wang E, Mei W N, Lu J, Li Y and Nagase S 2011 *Phys. Rev.* B **84** 075439
[12] Long M, Tang L, Wang D, Li Y and Shuai Z 2011 *ACS Nano* **5** 2593
[13] Pan L D, Zhang L Z, Song B Q, Du S X and Gao H J 2011 *Appl. Phys. Lett.* **98** 173102
[14] Son Y W, Cohen M L and Louie S G 2006 *Phys. Rev. Lett.* **97** 216803
[15] Deng H X, Li S S and Li J 2010 *J. Phys. Chem.* C **114** 4841
[16] Topsakal M, Cahangirov S and Ciraci S 2010 *Appl. Phys. Lett.* **96** 091912
[17] Zhang Y, Wen Y H, Zheng J C and Zhu Z Z 2009 *Appl. Phys. Lett.* **94** 113114
[18] Kang J, Li J, Wu F, Li S S and Xia J B 2011 *J. Phys. Chem.* C **115** 20466
[19] Khoo K H, Mazzoni M S C and Louie S G 2004 *Phys. Rev.* B **69** 201401
[20] Park C H and Louie S 2008 *Nano Lett.* **8** 2200
[21] Zhang Z and Guo W 2008 *Phys. Rev.* B **77** 075403
[22] Yilmaz H, Weiner B and Morell G 2010 *Phys. Rev.* B **81** 041312
[23] Ishigami M, Sau J D, Aloni S, Cohen M and Zettl A 2005 *Phys. Rev. Lett.* **94** 056804
[24] Takenobu T, Murayama Y and Iwasa Y 2006 *Appl. Phys. Lett.* **89** 263510
[25] Neugebauer J and Scheffler M 1992 *Phys. Rev.* B **46** 16067
[26] Blöchl P E 1994 *Phys. Rev.* B **50** 17953
[27] Kresse G and Joubert D 1999 *Phys. Rev.* B **59** 1758
[28] Kresse G and Hafner J 1993 *Phys. Rev.* B **47** 558
[29] Kresse G and Furthmüller J 1996 *Phys. Rev.* B **54** 11169
[30] Perdew J P, Burke K and Ernzerhof M 1996 *Phys. Rev. Lett.* **77** 3865
[31] White C T, Li J, Gunlycke D and Mintmire J W 2007 *Nano Lett.* **7** 825
[32] Lin Y M, Perebeinos V, Chen Z and Avouris P 2008 *Phys. Rev.* B **78** 161409
[33] Zheng F, Liu Z, Wu J, Duan W and Gu B L 2008 *Phys. Rev.* B **78** 085423